



**HAL**  
open science

# Interfacial protein adsorption behavior can be connected across a wide range of timescales using the microfluidic EDGE (Edge-based droplet GEneration) tensiometer

Tatiana Porto Santos, Boxin Deng, Meinou Corstens, Claire Berton-Carabin,  
Karin Schroën

## ► To cite this version:

Tatiana Porto Santos, Boxin Deng, Meinou Corstens, Claire Berton-Carabin, Karin Schroën. Interfacial protein adsorption behavior can be connected across a wide range of timescales using the microfluidic EDGE (Edge-based droplet GEneration) tensiometer. *Journal of Colloid and Interface Science*, 2024, 674, pp.951-958. 10.1016/j.jcis.2024.06.200 . hal-04698280

**HAL Id: hal-04698280**

**<https://hal.inrae.fr/hal-04698280v1>**

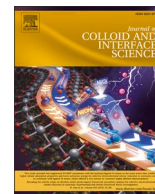
Submitted on 16 Sep 2024

**HAL** is a multi-disciplinary open access archive for the deposit and dissemination of scientific research documents, whether they are published or not. The documents may come from teaching and research institutions in France or abroad, or from public or private research centers.

L'archive ouverte pluridisciplinaire **HAL**, est destinée au dépôt et à la diffusion de documents scientifiques de niveau recherche, publiés ou non, émanant des établissements d'enseignement et de recherche français ou étrangers, des laboratoires publics ou privés.



Distributed under a Creative Commons Attribution 4.0 International License



## Regular Article

# Interfacial protein adsorption behavior can be connected across a wide range of timescales using the microfluidic EDGE (Edge-based droplet Generation) tensiometer

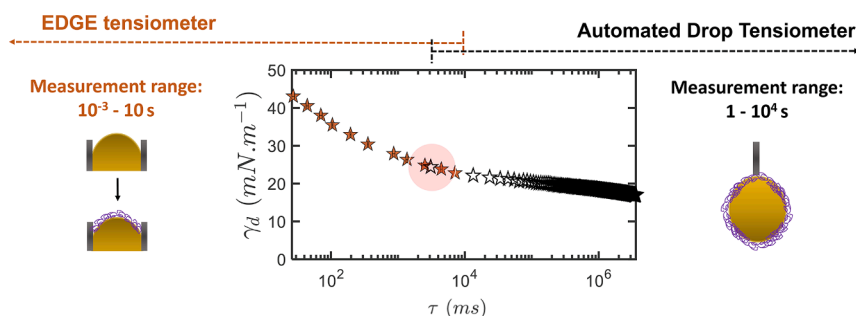
Tatiana Porto Santos<sup>a,\*</sup>, Boxin Deng<sup>a</sup>, Meinou Corstens<sup>a</sup>, Claire Berton-Carabin<sup>a,b</sup>, Karin Schroën<sup>a,\*</sup>

<sup>a</sup> Wageningen University and Research, Laboratory of Food Process Engineering, Bornse Weiland 9, 6708 WG Wageningen, the Netherlands

<sup>b</sup> INRAE, UR BIA, Nantes, 44000, France



## GRAPHICAL ABSTRACT



## ARTICLE INFO

## Keywords:

Dynamic interfacial tension  
Surface tension  
Microfluidics  
Short timescale  
Partitioned-EDGE  
Whey protein isolate  
Oil-in-water  
Air-in water  
Emulsions  
Foams

## ABSTRACT

**Hypothesis:** Our hypothesis is that dynamic interfacial tension values as measured by the partitioned-Edge-based Droplet Generation (EDGE) tensiometry can be connected to those obtained with classical techniques, such as the automated drop tensiometer (ADT), expanding the range of timescales towards very short ones.

**Experiments:** Oil-water and air-water interfaces are studied, with whey protein isolate solutions (WPI, 2.5 – 10 wt %) as the continuous phase. The dispersed phase consists of pure hexadecane or air. The EDGE tensiometer and ADT are used to measure the interfacial (surface) tension at various timescales. A comparative assessment is carried out to identify differences between protein concentrations as well as between oil-water and air-water interfaces.

**Findings:** The EDGE tensiometer can measure at timescales down to a few milliseconds and up to around 10 s, while the ADT provides dynamic interfacial tension values after at least one second from droplet injection and typically is used to also cover hours. The interfacial tension values measured with both techniques exhibit overlap, implying that the techniques provide consistent and complementary information. Unlike the ADT, the EDGE tensiometer distinguishes differences in protein adsorption dynamics at protein concentrations as high as 10 wt% (which is the highest concentration tested) at both oil-water and air-water interfaces.

\* Corresponding authors at: Wageningen University and Research, Laboratory of Food Process Engineering, Bornse Weiland 9, 6708 WG Wageningen, The Netherlands.

E-mail addresses: [tatiana.portodossantos@wur.nl](mailto:tatiana.portodossantos@wur.nl) (T. Porto Santos), [karin.schroen@wur.nl](mailto:karin.schroen@wur.nl) (K. Schroën).

<https://doi.org/10.1016/j.jcis.2024.06.200>

Received 8 May 2024; Received in revised form 13 June 2024; Accepted 25 June 2024

Available online 26 June 2024

0021-9797/© 2024 The Authors. Published by Elsevier Inc. This is an open access article under the CC BY license (<http://creativecommons.org/licenses/by/4.0/>).

## 1. Introduction

Emulsions are extensively employed in a variety of food products and consist of at least two immiscible phases – namely aqueous and oil. The most common food emulsions contain oil droplets dispersed in a water phase so-called oil-in-water (O/W) emulsions [20,24,39]. The emulsification process initiates droplet formation (accompanied by an increase in the interfacial area), leading to an increase in the Gibbs free energy of the system. This generates a driving force for re-coalescence that can be prevented by the use of emulsifiers that allow the decrease of interfacial tension ( $\gamma$ ), and thus the free energy. The stabilization of the droplets thereby occurs when these emulsifiers adsorb at the droplet interface [4,24,39]. The competing processes of droplet formation and re-coalescence, in case of insufficiently fast droplet stabilization, are highly dynamic and occur at inherently short timescales (in the order of sub-seconds) [34,39]. For instance, in industrial processes that rely on high-pressure homogenization systems, this timescale is  $\sim 0.1$ – $30$  ms [35].

This underscores the critical importance of understanding early effects occurring at the interface to eventually arrive at stable emulsion design. The dynamic interfacial tension ( $\gamma_d$ ) is indicative of these effects and changes over time. This influences not only the droplet size (during droplet formation and re-coalescence) but also, through that, the bulk properties (e.g., rheological properties) of an emulsion [7,21,24]. Thus, measurement of the dynamic interfacial tension of ingredients (especially of natural origin such as food proteins) at timescales relevant to industrial processes is a first crucial step in assessing emulsifier properties for stable emulsion production.

Typically, food emulsions and products contain proteins within a concentration range of 0.5 – 10 % [4,16,32,37] and the emulsification process is extremely fast. The main drawback of existing dynamic interfacial tension measurement methods is that the required time to record the first measurement is long when compared to large-scale emulsification processes. In an automated drop tensiometer (ADT), the measurement typically starts after slightly less than a second [3], which hampers the acquisition of early-stage interfacial effects. Moreover, it cannot distinguish effects created by the use of high emulsifier concentrations, resulting in the same ‘equilibrium’ interfacial tension value. This highlights the need of developing innovative techniques capable of measuring dynamic interfacial tension under relevant process and product conditions.

To address these challenges, researchers have explored microfluidic methods for measuring interfacial, and surface tension [6,8,14,19,22,36,40,43]. Within our research group, the microfluidic partitioned-Edge-based Droplet GEneration chip (partitioned-EDGE, hereafter referred to as EDGE) plays a special role. As introduced by Deng et al. [9], this micro-tensiometer is based on a balance between two opposing forces, namely the Laplace pressure of the confined interface and the external pressure applied into the system. Droplet formation takes place when the externally applied pressure exceeds the Laplace pressure, which is determined by emulsifier adsorption [10,24]. The droplet formation frequency as a function of applied external pressure can be used to determine the dynamic interfacial tension at very short timescales [10].

The EDGE tensiometer has been used for fast-adsorbing surfactants (i.e., the low molecular weight sodium dodecyl sulfate) [10]. In the current study, we expand its use to whey protein isolate (WPI), a commonly protein emulsifier, and validate the findings with ADT results at complementary timescales. Furthermore, we explore if the EDGE tensiometer could distinguish effects occurring at high WPI concentrations (2.5 – 10 wt%) that cannot be distinguished using classical techniques. Finally, we compare the outcomes obtained at the oil–water and air–water interface. In doing so, we gain unique insights into interfacial behavior.

## 2. Materials and methods

### 2.1. Materials

The dispersed phase consists of hexadecane (>99 %, Alfa Aesar, USA) stripped with alumina powder (MP EcoChrom ALUMINA N – Super I, Biomedicals) to remove impurities, or of air. Whey protein isolate (WPI, purity 97.0–98.4 %, BiPro®, Davisco, Switzerland) solutions are prepared in deionized water (Milli-Q, Merck Millipore) at concentrations ranging from 2.5 to 10 wt%. These WPI solutions serve as the continuous phase of the emulsions or foams. Tween 20 (2-[2-[3,4-bis(2-hydroxyethoxy)oxolan-2-yl]-2-(2-hydroxyethoxy)ethoxy]ethyl dodecanoate, P1379,  $\geq 40$  %, Sigma-Aldrich, USA) is also applied as the continuous phase of oil-in-water systems for comparative purposes. Prior to experimentation, the aqueous solutions are filtered using 0.22  $\mu\text{m}$  PES (polyethersulfone) filters (Merck, Ireland). Chip cleaning procedures involve the use of ethanol (96 % v/v, VWR International B.V., the Netherlands) and piranha solution (3:1 v/v ratio of sulfuric acid, purity 96 % (Sigma-Aldrich, USA) to 35 wt% hydrogen peroxide (Sigma-Aldrich, USA)). All chemicals are of analytical grade.

### 2.2. Microfluidic EDGE tensiometer

Custom-designed EDGE (Fig. 1a) microfluidic chips are produced by Micronit Microtechnologies B.V. (Enschede, the Netherlands). These chips consist of two primary sections: (1) two deep channels and (2) a shallow plateau housing an array of pores where droplets (or bubbles) spontaneously form [33,38]. The deep channels carry the dispersed (hexadecane or air, straight channel) and continuous (WPI solution, meandering channel) phases, as depicted in Fig. 1a. As illustrated in Fig. 1b, the deep channels with height  $H$  175  $\mu\text{m}$  (and width of 400  $\mu\text{m}$ ) are interconnected by the shallow plateau with length  $L$  200  $\mu\text{m}$  and width  $W$  500  $\mu\text{m}$ . This plateau is further partitioned into twelve parallel pores, each with a length, width, and height ( $l$ ,  $w$ ,  $h$ ) of 40, 20 and 1  $\mu\text{m}$ , respectively.

The EDGE chip is connected to the dispersed and continuous phases via tubing (Polyetheretherketone (PEEK), 0.75 mm, BGB®, Switzerland) and assembled in a chip holder (Fluidic Connect 4515, Micronit Microfluidics). The entire assembly is positioned in an inverted microscope (Axiovert 200 MAT, Carl Zeiss B.V., the Netherlands). In the experiment, the chip outlet for the dispersed phase is closed (“Closed” in Fig. 1a). The dispersed and continuous phases are pressurized using a digital pressure controller (Elveflow®, France) towards the chip inlets with pressures  $P_d$  and  $P_c$ , respectively. The effective pressure difference across the plateau region  $P_d^* = P_d - P_c/2$ , where  $P_c/2$  is the pressure halfway in the meandering channel.  $P_c$  is kept constant at 100 mbar, while  $P_d$  is varied to capture a comprehensive dataset as detailed in the Results and discussion section. In the section Measurement principle, details on the measurements are described.

#### 2.2.1. Measurement principle

The measurement principle of the EDGE tensiometer has been introduced by Deng et al. [10] to study the dynamic interfacial (and surface) tension of surfactant-stabilized droplets (and bubbles) [10]. For simplicity we will use “interfacial” tension regardless of the interface (oil–water or air–water). In essence, the measurement of interfacial tension ( $\gamma$ ) in the EDGE tensiometer relies on the formation of either droplets or bubbles, which is determined by the Laplace pressure of the confined meniscus in the pores ( $\Delta P_{L,pore}$ ).

$$\Delta P_{L,pore} = \gamma \left( \frac{1}{R_1} + \frac{1}{R_2} \right) \quad (1)$$

in which,  $R_1$  and  $R_2$  are the principal radii of curvature for the top and head-on view corresponding to half the pore width and height (Fig. 1c, top and bottom), respectively.

Droplet or bubble formation is determined by a balance between the  $\Delta P_{L,pore}$  and the externally applied pressure ( $P_d^*$ ). This means that above a certain  $P_d^*$ , the meniscus moves forward, causing droplets to grow and pinch-off. The droplet formation frequency ( $f_0$ ) is determined by the rate at which the emulsifier lowers  $\gamma$  (and thus  $\Delta P_{L,pore}$ ) (Equation (1)). At  $\Delta P_{L,pore} = P_d^*$ , Equation (1) can be reformulated as Equation (2), leading to values of dynamic interfacial tension ( $\gamma_d$ ) as they occur at the moment the meniscus starts to move. Since the timescale for droplet formation ( $\tau$ ) is governed by the time required for emulsifier adsorption, this implies that this timescale relates to the droplet formation frequency ( $\tau = 1/f_0$ ) [10]. By conducting a series of experiments with varied  $P_d^*$ , it is possible to assess the dynamic interfacial tension ( $\gamma_d$ ) as a function of adsorption time ( $\tau$ ). The experiments are carried out at room temperature. For more in-depth information on the underlying mechanisms, we refer to a previous publication from Deng et al. [10].

$$\gamma_d = P_d^* \left( \frac{1}{R_1} + \frac{1}{R_2} \right) \tag{2}$$

Additionally, we should highlight that there is a finite contact angle that the liquids have with the glass chip, and that can be taken into account by incorporating the contact angle  $\theta$  (Fig. 1c) in  $R_1 = w/2\cos(\theta)$  and  $R_2 = h/2\cos(\theta)$ . This leads to:

$$\gamma_d = \frac{P_d^*}{2} \left( \frac{wh}{(w+h)\cos(\theta)} \right) \tag{3}$$

Deng et al. [10] took  $\theta = 15^\circ$ , and here we confirm, as shown in Supplementary Information S1,  $\theta \sim 20^\circ$ .

### 2.3. Data treatment

Images and videos are recorded using a high-speed camera (FAST-CAM SA-Z, Photron Limited, Japan) with PFV4 software (Photron). Generally, the frame rate is set as 100,000 frames per second (fps) and specifically at 5,000 fps for low applied pressures  $P_d^*$  (to extend the accessible timescales). Three independent observations are analyzed to acquire the droplet formation frequency, which subsequently is used to determine the averaged adsorption (or formation) time over the triplicates using  $\tau = 1/f_0$ .

### 2.4. Automated drop tensiometer (ADT)

The automated drop tensiometer (ADT, Tracker, Teclis, Longessaigne, France) is used to measure rising droplets or bubbles formed at the tip of a needle immersed in a cuvette filled with WPI (or Tween 20) solution. The interfacial tension is recorded for at least 1 h at room temperature in duplicates. A representative curve is shown in this paper, but complementary data can be found in the publicly available repository.

## 3. Results and discussion

### 3.1. Proof-of-concept: EDGE vs. ADT

#### 3.1.1. Can the EDGE tensiometer complement ADT measurements?

In the EDGE tensiometer, the interfacial tension follows from the droplet formation frequency obtained at an externally applied pressure (as elaborated in *Measurement principle* above). Proteins continuously lower the dynamic interfacial tension until the applied pressure exceeds the Laplace pressure and a droplet is formed. The upper-boundary of the EDGE measurements (Fig. 2a) is set by the interfacial tension of a bare interface, which is dependent on the components used (e.g., type of oil). The equilibrium interfacial tension of a saturated interface sets the lower-boundary of the measurement (Fig. 2a), and that depends on the emulsifier type, and concentration used.

To illustrate the complementary nature of the EDGE tensiometer and ADT across a broad range of timescales, we plot the dynamic interfacial tension,  $\gamma_d$ , against the adsorption time,  $\tau$ , for WPI (2.5 – 10 wt%) and a surfactant (Tween 20, 0.5 and 2 wt%) (Fig. 2b) against hexadecane. These results show that irrespective of the emulsifier used, the results obtained by the ADT connect well with the EDGE measurements. Fig. 2b also shows that Tween 20 exhibits a faster adsorption and a more significant reduction in interfacial tension through its higher adsorption energy per surface area [5,13].

To better compare the results of ADT and EDGE in Fig. 2b a small nuance needs to be made. The ADT measurement relies on analysis of the shape and dimension of a suspended droplet [2,4,27], and for that droplet to be formed (injected), a finite amount of time is needed, after which the actual measurement starts (and this latter time is recorded).

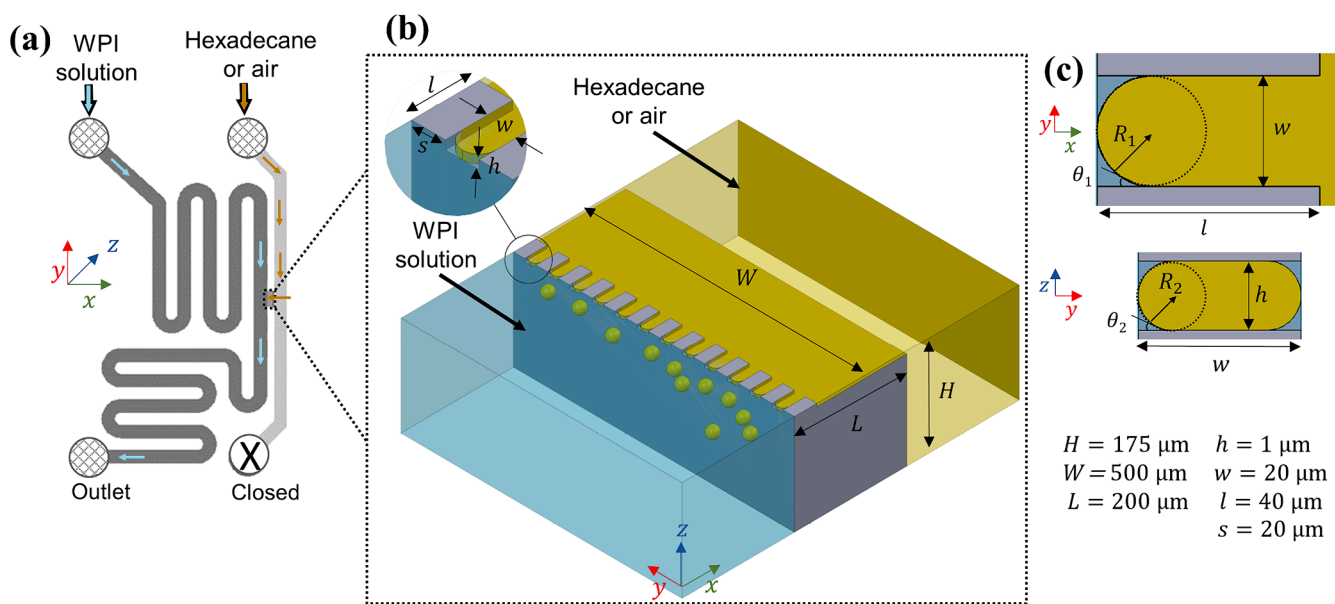


Fig. 1. EDGE chip: (a) schematic representation (not to scale) of the setup (b) zooming in on the shallow plateau with the pore region. (c, top) and (c, bottom) are the schematic top and head-on view of one pore, respectively.  $R_1$  and  $R_2$  are the two principle radii of curvature across the meniscus. The flow direction of the continuous and dispersed phases is shown in (a) and (b) and the channel dimensions are in the bottom right region of the figure.

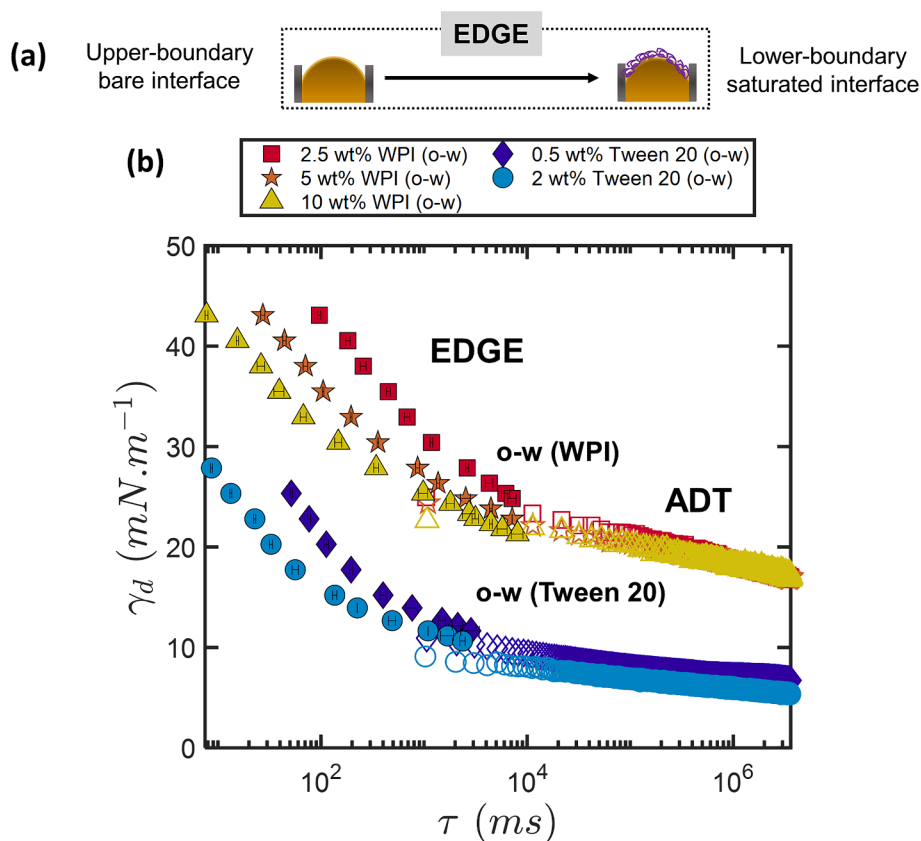


Fig. 2. (a) Schematic representation of the upper- and lower-boundary of EDGE measurements and (b) dynamic interfacial tension ( $\gamma_d$ ) as a function of adsorption time ( $\tau$ ) at the oil-water (o-w) interface for 2.5–10 wt% WPI and 0.5–2 wt% Tween 20. Data points on the left are those acquired using EDGE (filled symbols), while on the right are those obtained with ADT (unfilled symbols).

During this substantial ‘lag time’ of a few seconds needed to achieve the pre-defined droplet volume, emulsifier adsorption takes place. In the EDGE tensiometer, interfacial tension is measured without delay, and this difference can be taken into account as explained next.

The lag time (or injection time) can be factored into the “real” adsorption time ( $\tau$ ). The injection time is influenced by the experimental conditions (e.g., the inner phase viscosity and droplet size). Here, we use injection times of 2000 ms (Fig. 3b) and 6000 ms (Fig. 3c), which are

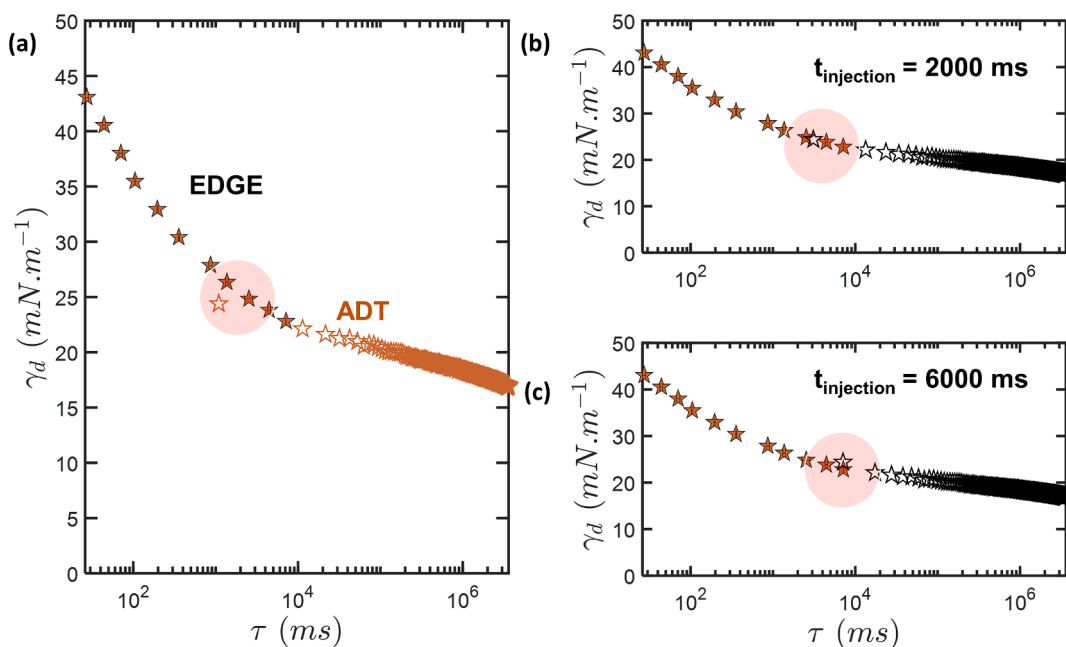


Fig. 3. (a) Dynamic interfacial tension ( $\gamma_d$ ) as a function of adsorption time ( $\tau$ ) at the oil-water (o-w) interface for 5 wt% WPI. (b)(c) The differences in the injection time ( $t_{injection}$ ) are shown. The orange circles highlight the region where a difference in adsorption time, due to different injection times, can be observed.

both within the experimentally observed range to illustrate the possible effect this may have. Essentially, this shifts the ADT data to the right (Fig. 3bc) compared to the unadjusted data (Fig. 3a). When using a time delay of 2 s, our data seamlessly connect, which is an improvement compared to results presented in a previous publication [10]. To reduce the offset between the techniques another experimental aspect has to be considered. When new droplets are injected in the ADT, part of the previous droplet remains at the tip of the needle, which may contain an initial load of adsorbed molecules that will be later transferred to the newly injected droplet. Therefore, as we have considered in our experiments, we suggest to always generate and discard some droplets before the actual measurement starts.

The high protein concentration used in the present study ensures that diffusion is relatively fast and thus emulsifier incorporation at the oil–water interface is governed by emulsifier adsorption and not limited by mass transfer effects [44]. This is substantiated through calculations of characteristic timescales (Supplementary Information S2) [1,18,19,39,41], showing that emulsifier adsorption kinetics at the interface (characterized by the characteristic timescales for adsorption,  $t_{ads}$ ), is always orders of magnitude larger than emulsifier diffusion (determined by the characteristic timescales for diffusion,  $t_{diff}$ ) through the bulk phase towards the sub-interface. We conclude that for the systems under study, the adsorption time and thus the interfacial tension values found are independent of the system-specific characteristics i.e., dimensions of the measurement system, for high protein concentrations (2.5 – 10 wt%). This ensures that EDGE and ADT interfacial tension values at similar timescales will be the same as sufficient proteins are in the vicinity of the interface when the measurement initiates ( $t_{diff} < 1$  ms, Supplementary Information S2) because of the relatively high rate of diffusion [23]. The situation is expected to be different at very low emulsifier concentrations. As shown for sodium dodecyl sulfate and proteins, diffusion-controlled mass transfer may become dominant at very low concentration [4,10], which accentuates the importance of droplet size. For small droplets (increased curvature), relatively high amounts of proteins are available per unit area [1,18,30], which will influence the interfacial tension values obtained by both techniques at similar timescales.

We conclude that EDGE and ADT serve as complementary techniques for comprehensively evaluating the interfacial behavior of emulsifiers at high emulsifier concentrations across various timescales. EDGE captures the adsorption process down to a few milliseconds ( $\sim 5$  ms in this work) and up to around 10 s, while ADT provides measurements in the seconds to hours range (Fig. 3).

### 3.2. EDGE measurements: Early effects of proteins at the interface

#### 3.2.1. Oil-water interface

Our focus next shifted to distinguishing the effect of (high) protein concentrations at the oil–water interface (Fig. 4ab). The EDGE measurements ( $\gamma_d$  vs.  $\tau$  plots, Fig. 4a) allow to distinguish the effect of (high) protein concentrations (2.5 to 10 wt%) at short timescales. For example, to achieve  $\gamma \sim 40$  mN.m<sup>-1</sup>, 15 ms are needed at 10 wt% WPI, while this time increases to 44 and 181 ms at 5 and 2.5 wt%, respectively. In Fig. 4a, we see a relatively linear initial decrease in interfacial tension as function of the logarithmic droplet formation time, followed by a less sharp decrease. Where the transition takes place depends on the protein concentration, as indicated by the vertical lines. This is reflecting changes in adsorption dynamics [4,26] induced by saturation of the interface that increases the barrier for emulsifier adsorption [11], possibly together with early protein network formation as reported for WPI solutions ( $\lesssim 0.1$  %w/v) to occur at sub-second timescales [17]. However, unlike EDGE that is diffusion-based, the rheology chip used in the work of Hinderink et al. [17] is convection-based with mass transport, and thus film formation, occurring because of this [28].

It is important to point out that proteins might take extremely long times to reach equilibrium due to constant conformational changes and rearrangements at the oil–water interface. Often such equilibrium is not even achieved [4,13]. This time consuming scenario influences the accessible range of interfacial tensions (e.g., the low end in EDGE measurements). Because of this, it is not feasible to measure at ‘equilibrium Laplace pressure’ with the EDGE device. Still, we achieve a minimum interfacial tension of  $\sim 21$  mN.m<sup>-1</sup>, which is higher than the interfacial tension found by ADT ( $\sim 17$  mN.m<sup>-1</sup> after 1 h of measurement for WPI 2.5 – 10 wt%), but in a quite similar range.

For ADT, as pointed out earlier, the measurement starts at relatively long timescales, thus the values found for the different concentrations are very similar due to the high surface coverage (Fig. 4b). Changes in interfacial tension in time are related to conformational changes and entanglements of the adsorbed layer [4,26]. This makes the ADT measurement not well-suited to observe differences in adsorption kinetics at the high WPI concentrations used (Fig. 4b), while EDGE is very capable of doing so.

#### 3.2.2. Air-water interface

In addition to the oil–water interface, we apply the EDGE tensiometer to obtain insights in the dynamics of WPI at the air–water interface (Fig. S2, Supplementary Information S3). To fairly compare these interfaces, we examine the interfacial pressure ( $\pi = \gamma_0 - \gamma_d$ ) (Fig. 5a) which removes the disparity of the tension values of pure oil- and air–water interfaces ( $\gamma_0$ ,  $\sim 44$  mN.m<sup>-1</sup> for hexadecane-water and  $\sim 72$

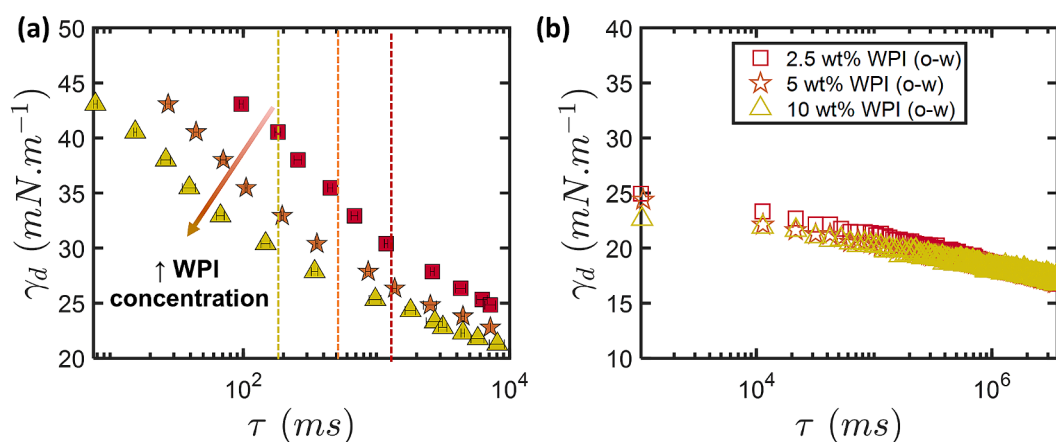


**Fig. 4.** Dynamic interfacial tension ( $\gamma_d$ ) as a function of adsorption time ( $\tau$ ) at the oil–water (o-w) interface for a range of WPI concentrations (2.5 – 10 wt%) acquired using (a) EDGE and (b) ADT. The vertical dashed lines in (a) indicate the change in the slope of the curves.

$\text{mN}\cdot\text{m}^{-1}$  for air–water) [4,24]. To normalize the data, we use values relative to that of the bare interface value,  $\gamma_d/\gamma_0$  (Fig. 5b).

For all concentrations, we find similar trends for the oil–water and air–water interface (Fig. 5a), with the air–water interface exhibiting slightly higher normalized  $\pi$  values at low timescales. We hypothesize that the air–water interface facilitates an easier spread of the protein molecules due to the higher driving force, and that at the oil–water interface additional oil-emulsifier interactions may come into play. At longer timescales, the normalized  $\pi$  is higher for the oil–water interface [12,25,29,31], which is expected due to non-polar segments of the proteins intruding into the oil phase [5,12]. The cross-over point where the surface pressure of the two systems is the same (within the blue box region in Fig. 5a) shifts to shorter timescales at increasing protein concentration. This is logically related to interface saturation effects. Still, if these were the only effects playing a role, the transition would take place at the same normalized surface pressure, and that is not the case. It is expected that protein configuration and the timescale for protein ‘nesting’ at the interface starts playing a role. Indeed, different bulk protein concentrations may lead to distinct protein configuration at the interface as more unfolding is expected at low protein concentration [26,42]. Moreover, at the very short timescales used, protein rearrangement and intrusion into the oil phase have not had a lot of time to occur, and they will be different for the two systems.

To the best of our knowledge, it is the first time that these differences are reported to play a role at timescales as short as 10–1000 ms. From Fig. 5b, it is also clear that the rearrangement and unfolding of the protein molecules can take place to an even higher extent within the oil phase [4,5], as is reflected in the greater normalized effect on surface pressure at much longer timescales.

The findings obtained with the EDGE tensiometer hold significant relevance in the context of food production. Currently, proteins are often used at high concentrations to mitigate droplet re-coalescence, ensuring small droplet size, and through that high physical stability with a lot of the protein remaining in the bulk phase. By scrutinizing the dynamics of protein movement towards the interface, i.e., the interfacial tension

decrease, a more judicious selection of protein concentration (to promote rapid emulsion stabilization by suppressing re-coalescence) as well as protein source becomes feasible. We should also highlight that other microfluidic strategies (i.e., Y-junctions) have been used to assess the dynamic interfacial tension, but rarely for proteins, or even high protein concentrations (e.g., whey protein solutions up to 0.5 % [15]). The EDGE tensiometer thereby emerges as a valuable and practical tool to predict and eventually control protein-stabilizing mechanisms at oil- and air–water interfaces.

#### 4. Conclusions

Early-on assessment of protein adsorption at fluid interfaces is of utmost importance, but classical techniques to assess dynamic interfacial tension (such as automated drop tensiometer, ADT) fall short in determining this property at the very short timescales relevant for food production. This is one of the reasons recent studies have applied microfluidic methods for measuring interfacial, and surface tension at short timescales [6,8,14,19,22,36,40,43]. In our group, we have successfully achieved such short timescale measurements (from the millisecond range up to tens of seconds) by using the novel EDGE (Edge-based Droplet GEneration) tensiometer [10].

The measurement in the EDGE device is based on one force exceeding another, namely the Laplace pressure of the confined interface (which is reduced in time due to adsorption) and the external pressure applied onto the system that at some point in time exceeds the Laplace pressure. In the current study, we not only tested the ability of the EDGE device to measure both interfacial and surface tension but also connected its results to those acquired using ADT at similar timescales, both for typical food proteins and surfactants. We consider this a significant step toward better understanding of processes as they occur during emulsion formation (EDGE), as well as long-term stability (ADT), and how to connect them. Unlike the ADT, the EDGE tensiometer is also able to distinguish dynamic interfacial effects created by high protein concentrations, at both oil–water and air–water interface.

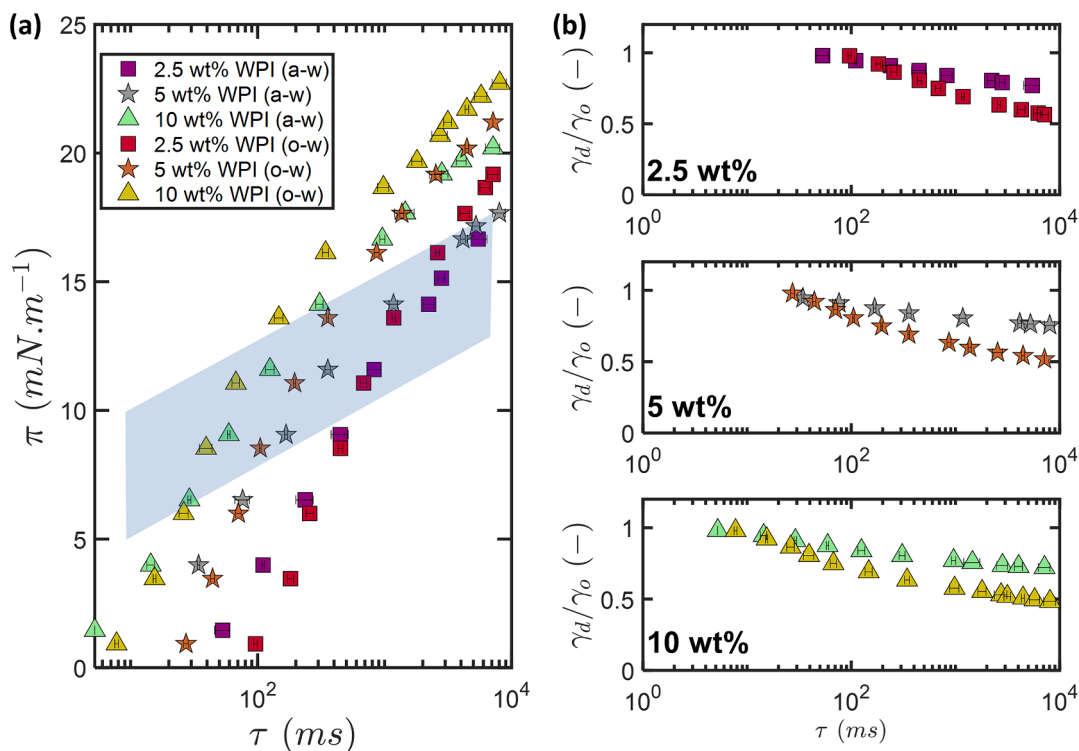


**Fig. 5.** (a) Surface pressure ( $\pi$ ) and (b) interfacial tension normalized ( $\gamma_d/\gamma_0$ ) as a function of adsorption time ( $\tau$ ) at air–water (a-w) and oil–water (o-w) interfaces for a range of WPI concentrations (2.5 – 10 wt%). The blue box in (a) indicates a transition region detailed in the text. The surface pressure is defined as  $\pi = \gamma_0 - \gamma_d$ .

To summarize, this study opens a window of opportunity for assessing the adsorption kinetics of ingredients that are often present at high concentrations in food products and to do so at timescales as encountered in industrial processes. For future studies, we envision to further validate the applicability of the EDGE tensiometer by comparing its outcomes with those of other classical techniques such as e.g., the bubble pressure tensiometry for air–water systems. Furthermore, we will explore in how far the EDGE tensiometer can be used to evaluate e.g., water-in-oil emulsions (for that the device would need to be hydrophobized), and that is highly relevant for other domains such as chemical, petroleum, and pharma industries.

### CRedit authorship contribution statement

**Tatiana Porto Santos:** Writing – original draft, Visualization, Validation, Methodology, Investigation, Funding acquisition, Formal analysis, Data curation, Conceptualization. **Boxin Deng:** Writing – review & editing, Visualization, Validation, Methodology, Investigation, Formal analysis, Conceptualization. **Meinou Corstens:** Writing – review & editing, Methodology, Conceptualization. **Claire Berton-Carabin:** Writing – review & editing, Methodology, Conceptualization. **Karin Schroën:** Writing – review & editing, Supervision, Methodology, Funding acquisition, Conceptualization.

### Declaration of competing interest

The authors declare that they have no known competing financial interests or personal relationships that could have appeared to influence the work reported in this paper.

### Data availability

The data associated to this publication can be found in the 4TU data repository [4TU.Research-Data, URL: <https://doi.org/10.4121/d4c5feca-4e5c-44fe-a358-55ae9cc09100>].

### Acknowledgements

This work is funded by the European Union HORIZON MSCA Post-doctoral Fellowships, under Grant Agreement 101062730 (EVALUATOR). Views and opinions expressed are however those of the authors only and do not necessarily reflect those of the European Union or the Research Executive Agency. Neither the European Union nor the granting authority can be held responsible for them.

### Appendix A. Supplementary data

Supplementary data to this article can be found online at <https://doi.org/10.1016/j.jcis.2024.06.200>.

### References

- N.J. Alvarez, L.M. Walker, S.L. Anna, Diffusion-limited adsorption to a spherical geometry: The impact of curvature and competitive time scales, *Phys. Rev. E Stat. Nonlinear Soft Matter Phys.* 82 (2010) 011604, <https://doi.org/10.1103/PhysRevE.82.011604>.
- J.D. Berry, M.J. Neeson, R.R. Dagastine, D.Y.C. Chan, R.F. Tabor, Measurement of surface and interfacial tension using pendant drop tensiometry, *J. Colloid Interface Sci.* 454 (2015) 226–237, <https://doi.org/10.1016/j.jcis.2015.05.012>.
- C.C. Berton-Carabin, L. Sagis, K. Schroën, Formation, structure, and functionality of interfacial layers in food emulsions, *Annu. Rev. Food Sci. Technol.* 9 (2018) 551–587, <https://doi.org/10.1146/annurev-food-030117-012405>.
- C.J. Beverung, C.J. Radke, H.W. Blanch, Protein adsorption at the oil/water interface: characterization of adsorption kinetics by dynamic interfacial tension measurements, *Biophys. Chem.* 81 (1999) 59–80, [https://doi.org/10.1016/S0301-4622\(99\)00082-4](https://doi.org/10.1016/S0301-4622(99)00082-4).
- M.A. Bos, T. Van Vliet, Interfacial rheological properties of adsorbed protein layers and surfactants: a review, *Adv. Colloid Interface Sci.* 91 (2001) 437–471, [https://doi.org/10.1016/S0001-8686\(00\)00077-4](https://doi.org/10.1016/S0001-8686(00)00077-4).
- Q. Brosseau, J. Vignon, J.C. Baret, Microfluidic dynamic interfacial tensiometry ( $\mu$ DIT), *Soft Matter* 10 (2014) 3066–3076, <https://doi.org/10.1039/c3sm52543k>.
- C. Chung, D.J. McClements, Structure-function relationships in food emulsions: Improving food quality and sensory perception, *Food Struct.* 1 (2) (2014) 106–126, <https://doi.org/10.1016/j.foostr.2013.11.002>.
- R. D'Apolito, A. Perazzo, M. D'Antuono, V. Preziosi, G. Tomaiuolo, R. Miller, S. Guido, measuring interfacial tension of emulsions in situ by microfluidics, *Langmuir* 34 (17) (2018) 4991–4997, <https://doi.org/10.1021/acs.langmuir.8b00208>.
- B. Deng, K. Schroën, J. de Ruyter, Effects of dynamic adsorption on bubble formation and coalescence in partitioned-EDGE devices, *J. Colloid Interface Sci.* 602 (2021) 316–324, <https://doi.org/10.1016/j.jcis.2021.06.014>.
- B. Deng, K. Schroën, M. Steegmans, J. de Ruyter, Capillary pressure-based measurement of dynamic interfacial tension in a spontaneous microfluidic sensor, *Lab Chip* 22 (20) (2022) 3860–3868, <https://doi.org/10.1039/d2lc00545j>.
- J. Eastoe, J.S. Dalton, Dynamic surface tension and adsorption mechanisms of surfactants at the air–water interface, *Adv. Colloid Interface Sci.* 85 (2000) 103–144, [https://doi.org/10.1016/S0001-8686\(99\)00017-2](https://doi.org/10.1016/S0001-8686(99)00017-2).
- V.B. Fainerman, E.V. Aksenenko, N. Mucic, A. Javadi, R. Miller, Thermodynamics of adsorption of ionic surfactants at water/alkane interfaces, *Soft Matter* 10 (36) (2014) 6873–6887, <https://doi.org/10.1039/c4sm00463a>.
- A.L.R. Costa, R.L. Cunha, Impact of oil type and WPI/Tween 80 ratio at the oil–water interface: Adsorption, interfacial rheology and emulsion features, *Colloids Surf. B Biointerfaces* 164 (2018) 272–280, <https://doi.org/10.1016/j.colsurfb.2018.01.032>.
- H. Gu, M.H.G. Duits, F. Mugele, Interfacial tension measurements with microfluidic tapered channels, *Colloids Surf. A Physicochem Eng Asp* 389 (1–3) (2011) 38–42, <https://doi.org/10.1016/j.colsurfa.2011.08.054>.
- C. Güell, M. Ferrando, A. Trentin, K. Schroën, Apparent interfacial tension effects in protein stabilized emulsions prepared with microstructured systems, *Membranes* 7 (2) (2017), <https://doi.org/10.3390/membranes7020019>.
- E. Hebshy, M. Buffa, B. Guamis, A. Blasco-Moreno, A.J. Trujillo, Physical and oxidative stability of whey protein oil-in-water emulsions produced by conventional and ultra high-pressure homogenization: Effects of pressure and protein concentration on emulsion characteristics, *Innov. Food Sci. Emerg. Technol.* 32 (2015) 79–90, <https://doi.org/10.1016/j.ifset.2015.09.013>.
- E.B.A. Hinderink, J. de Ruyter, J. de Leeuw, K. Schroën, L.M.C. Sagis, C.C. Berton-Carabin, Early film formation in protein-stabilised emulsions: Insights from a microfluidic approach, *Food Hydrocoll.* 118 (2021), <https://doi.org/10.1016/j.foodhyd.2021.106785>.
- F. Jin, R. Balasubramaniam, K.J. Stebe, Surfactant adsorption to spherical particles: The intrinsic length scale governing the shift from diffusion to kinetic-controlled mass transfer, *J. Adhes.* 80 (9) (2004) 773–796, <https://doi.org/10.1080/00218460490480770>.
- M. Kalli, L. Chagot, P. Angeli, Comparison of surfactant mass transfer with drop formation times from dynamic interfacial tension measurements in microchannels, *J. Colloid Interface Sci.* 605 (2022) 204–213, <https://doi.org/10.1016/j.jcis.2021.06.178>.
- I. Kralova, J. Sjöblom, Surfactants used in food industry: A review, *J. Dispers. Sci. Technol.* 30 (9) (2009) 1363–1383, <https://doi.org/10.1080/01932690902735561>.
- M. L'Estimé, M. Schindler, N. Shahidzadeh, D. Bonn, Droplet size distribution in emulsions, *Langmuir* 40 (1) (2024) 275–281, <https://doi.org/10.1021/acs.langmuir.3c02463>.
- X. Liang, M. Li, K. Wang, G. Luo, Determination of Time-Evolving interfacial tension and ionic surfactant adsorption kinetics in microfluidic droplet formation process, *J. Colloid Interface Sci.* 617 (2022) 106–117, <https://doi.org/10.1016/j.jcis.2022.02.139>.
- M.J. Martinez, C.C. Sánchez, J.M.R. Patino, A.M.R. Pilosof, Interactions in the aqueous phase and adsorption at the air–water interface of caseinoglycomacropeptide (GMP) and  $\beta$ -lactoglobulin mixed systems, *Colloids Surf. B Biointerfaces* 68 (1) (2009) 39–47, <https://doi.org/10.1016/j.colsurfb.2008.09.006>.
- D.J. McClements, *Food emulsions: Principles, practices and techniques*, 3rd ed, CRC Press, 2015.
- K. Mędrzycka, W. Zwierzykowski, Adsorption of alkyltrimethylammonium bromides at the various interfaces, *J. Colloid Interface Sci.* 230 (1) (2000) 67–72, <https://doi.org/10.1006/jcis.2000.7045>.
- R. Miller, V. Fainerman, A. Makievski, J. Kragel, D. Grigoriev, V. Kazakov, O. Sinyachenko, Dynamics of protein and mixed protein/surfactant adsorption layers at the water/fluid interface, *Adv. Colloid Interface Sci.* 86 (2000) 39–82, [https://doi.org/10.1016/S0001-8686\(00\)00032-4](https://doi.org/10.1016/S0001-8686(00)00032-4).
- R. Miller, A. Hofmann, R. Hartmann, A. Halbig, K.-H. Schano, Measuring dynamic surface and interfacial tensions, *Adv. Mater.* 4 (5) (1992) 370–374, <https://doi.org/10.1002/adma.19920040513>.
- K. Muijlwijk, W. Huang, J.E. Vuist, C. Berton-Carabin, K. Schroën, Convective mass transport dominates surfactant adsorption in a microfluidic Y-junction, *Soft Matter* 12 (44) (2016) 9025–9029, <https://doi.org/10.1039/c6sm01677d>.
- P. Müller, D.J. Bonthuis, R. Miller, E. Schneck, Ionic surfactants at air/water and oil/water interfaces: A comparison based on molecular dynamics simulations, *J. Phys. Chem. B* 125 (1) (2021) 406–415, <https://doi.org/10.1021/acs.jpcc.0c08615>.
- S. Narayan, D.B. Moravec, B.G. Hauser, A.J. Dallas, C.S. Dutcher, Removing water from diesel fuel: Understanding the impact of droplet size on dynamic interfacial tension of water-in-fuel emulsions, *Energy Fuel* 32 (7) (2018) 7326–7337, <https://doi.org/10.1021/acs.energyfuels.8b00502>.



- [31] V. Pradines, V.B. Fainerman, E.V. Aksenenko, J. Krägel, N. Mucic, R. Miller, Adsorption of alkyl trimethylammonium bromides at the water/air and water/hexane interfaces, *Colloids Surf A Physicochem Eng Asp* 371 (1–3) (2010) 22–28, <https://doi.org/10.1016/j.colsurfa.2010.08.052>.
- [32] M. Primožic, A. Duchek, M. Nickerson, S. Ghosh, Effect of lentil proteins isolate concentration on the formation, stability and rheological behavior of oil-in-water nanoemulsions, *Food Chem.* 237 (2017) 65–74, <https://doi.org/10.1016/j.foodchem.2017.05.079>.
- [33] S. Sahin, K. Schroën, Partitioned EDGE devices for high throughput production of monodisperse emulsion droplets with two distinct sizes, *Lab Chip* 15 (11) (2015) 2486–2495, <https://doi.org/10.1039/c5lc00379b>.
- [34] K. Schroën, B. Deng, C. Berton-Carabin, S. Marze, M. Corstens, E. Hinderink, Microfluidics-based observations to monitor dynamic processes occurring in food emulsions and foams, *Curr. Opin. Food Sci.* 50 (2023) 100989, <https://doi.org/10.1016/j.cofs.2023.100989>.
- [35] S. Schultz, G. Wagner, K. Urban, J. Ulrich, High-pressure homogenization as a process for emulsion formation, *Chem. Eng. Technol.* 27 (4) (2004) 361–368, <https://doi.org/10.1002/ceat.200406111>.
- [36] M.L.J. Steegmans, A. Warmerdam, K.G.P.H. Schroen, R.M. Boom, Dynamic interfacial tension measurements with microfluidic Y-junctions, *Langmuir* 25 (17) (2009) 9751–9758, <https://doi.org/10.1021/la901103r>.
- [37] J. Suthar, A. Jana, S. Balakrishnan, High protein milk ingredients - a tool for value-addition to dairy and food products, *Journal of Dairy, Veterinary & Animal Research* 6 (1) (2017) 259–265, <https://doi.org/10.15406/jdvar.2017.06.00171>.
- [38] K.C. van Dijke, G. Veldhuis, K. Schroën, R.M. Boom, Simultaneous formation of many droplets in a single microfluidic droplet formation unit, *AIChE J* 56 (3) (2010) 833–836, <https://doi.org/10.1002/aic.11990>.
- [39] Walstra, Pieter. (2003). *Physical chemistry of foods* (Vol. 121). Marcel Dekker.
- [40] K. Wang, Y.C. Lu, J.H. Xu, G.S. Luo, Determination of dynamic interfacial tension and its effect on droplet formation in the T-shaped microdispersion process, *Langmuir* 25 (4) (2009) 2153–2158, <https://doi.org/10.1021/la803049s>.
- [41] K. Wang, L. Zhang, W. Zhang, G. Luo, Mass-Transfer-Controlled Dynamic Interfacial Tension in Microfluidic Emulsification Processes, *Langmuir* 32 (13) (2016) 3174–3185, <https://doi.org/10.1021/acs.langmuir.6b00271>.
- [42] R. Wüstneck, J. Krägel, R. Miller, V.B. Fainerman, P.J. Wilde, D.K. Sarker, D. C. Clark, Dynamic surface tension and adsorption properties of  $\beta$ -casein and  $\beta$ -lactoglobulin, *Food Hydrocoll.* 10 (4) (1996) 395–405, [https://doi.org/10.1016/S0268-005X\(96\)80018-X](https://doi.org/10.1016/S0268-005X(96)80018-X).
- [43] J.H. Xu, P.F. Dong, H. Zhao, C.P. Tostado, G.S. Luo, The dynamic effects of surfactants on droplet formation in coaxial microfluidic devices, *Langmuir* 28 (25) (2012) 9250–9258, <https://doi.org/10.1021/la301363d>.
- [44] A.-P. Wei, J.N. Herron, J.D. Andrade, D.J.A. Crommelin, H. Schellekens, *The role of protein structure in surface tension kinetics*, in: *From Clone to Clinic*, Vol. 1, Springer, 1990, pp. 305–313.